Available online at www.sciencedirect.com

ScienceDirect

journal homepage: www.jfda-online.com

Original Article

Electrochemistry and determination of cefdinir by voltammetric and computational approaches

CrossMark

İbrahim Hüdai Taşdemir*

Department of Chemistry, Faculty of Arts and Science, Amasya University, Amasya 05200, Turkey

ABSTRACT

The oxidation and reduction behavior of cefdinir (CEF) was studied by experimental methods and computational calculations at B3LYP/6-31+G (d)//AM1. Voltammetric studies were carried out based on two irreversible reduction peaks at approximately −0.5 and −1.2 V on a hanging mercury drop electrode (HMDE) and on one irreversible oxidation peak at approximately 1.0 V on a glassy carbon electrode (GCE) versus Ag/AgCl, KCl (3.0M) in Britton–Robinson (BR) buffer at pH 4.2 and 5.0, respectively. Differential pulse adsorptive stripping voltammetric methods have been developed and validated for determination of CEF in different samples. The linear range was established as 0.25–40.0 μM for HMDE and 0.40–10.0 μM for GCE. Limit of quantification was calculated to be 0.20 and 0.26 μM for HMDE and GCE, respectively. These methods were successfully applied to assay the drug in tablets and human serum with good recoveries between 92.7% and 107.3% having relative standard deviation less than 10%.

1. Introduction

Cefdinir (CEF), chemically known as [(6R,7R)-7-[[(2Z)-(2-amino-4-thiazolyl)(hydroxyl imino)acetyl]amino]-3-ethenyl-8-oxo-5-thia-1-azabicyclo[4.2.0]oct-2-ene-2-carboxylic acid] (Fig. 1), is a broad-spectrum oral third-generation cephalosporin that has been approved for the treatment of some kind of bacterial infections [1,2].

Many kind of analytical methods have been described for the determination of CEF in pharmaceutical samples and biological fluids, including high-performance liquid chromatography (HPLC)–tandem mass spectrometry [3], HPLC–solid-phase extraction [4,5], stability indicating chromatography [6,7], reverse-phase HPLC with UV deduction [8], different

kinds of liquid chromatography [9–13], resonance Rayleigh scattering spectra [14], and spectrophotometry [15,16]. Because the CEF molecule contains electroactive groups, reports have been published regarding its reduction behavior on mercury electrode [17–19]. It could be possible to evaluate the redox characteristics, adsorption–diffusion properties, and charge transfer mechanisms for electroactive molecules by electrochemical methods. These parameters and their evaluation are of great importance for distribution, metabolism, pharmacological, toxicological, and pharmacokinetic behaviors of drug molecules [17–25]. Theoretical calculations were also found to be useful as a value-added tool to enlighten oxidation–reduction mechanisms [22,23].

Voltammetric techniques are used for the quantitative determination of a variety of organic and inorganic
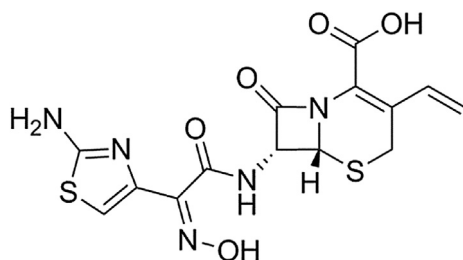
Fig. 1 – Chemical structure of cefdinir.

substances including drug-active ingredients and excipients in pharmaceutical dosage and their possible metabolites in biological fluids. In addition, voltammetric stripping technique extends the use of these methods ensuring lower detection limits. Many applications of voltammetric stripping methods have been reported in literature to determine environmentally and biologically important substances [17–33].

At present, there is no electrochemical study dealing with the oxidation behavior of CEF and its determination on carbon-based electrodes. This study was designed to investigate the reduction and oxidation behavior of CEF on both glassy carbon electrode (GCE) and hanging mercury drop electrode (HMDE). Tentative reaction mechanisms on both electrodes were also proposed. Computational studies were performed to enlighten the proposed mechanisms. In addition, it was also aimed to develop rapid, simple, and novel voltammetric methods for direct determination of CEF in pharmaceutical dosage forms and human serum.

2. Experimental analysis

2.1. Apparatus

All voltammetric measurements were carried out using a Gamry instruments framework electrochemical analyzer (reference 3000; Gamry Instruments, Warminster, PA, USA). The three-electrode system consisted of working electrodes (HMDE; BAS CGME 1108, 0.0145 cm^2, and GCE; BAS, MF 2012, 0.071 cm^2), reference electrode (Ag/AgCl; 3M KCl; MF-2052, RE-5B), and a Pt auxiliary electrode (BAS MW-1034). Before performing each experiment, GCE was polished manually with slurries prepared from 0.01-μm aluminum oxide on a smooth polishing pad (BAS velvet polishing pad), and then thoroughly rinsed with double-distilled water.

All pH measurements were obtained using Thermo Orion Model 720A pH ion meter having an Orion combined glass pH electrode (912600; Thermo Fisher Scientific). Double-distilled deionized water was obtained from an ultrapure water system (ELGA as PURELAB Option-S). All measurements were performed at room temperature (23 ± 2 °C).

2.2. Reagents and solutions

The CEF standard was purchased from Bilim Pharmaceuticals (Istanbul, Turkey). All chemicals used were of analytical grade and used as received.

The CEF stock solutions (5.0 mM) were prepared in absolute ethanol and kept in dark and stored at <4°C. Working CEF solutions were prepared by sufficient dilution of stock solution with supporting electrolyte having optimum pH and used within the same day to avoid decomposition. Phosphoric acid (Riedel-de-Haen, Honeywell Specialty Chemicals Seelze GmbH, Germany), boric acid (Riedel-de-Haen, Honeywell Specialty Chemicals Seelze GmbH, Germany), and acetic acid (Merck KGaA, Darmstadt, Germany) were used in the preparation of BR solution in which each component had an analytical concentration of 0.04 M. Double-distilled deionized water was used in preparing of all the solutions.

2.3. Procedure

For voltammetric measurements, a known volume of CEF solution was pipetted into a 10.0-mL supporting electrolyte. The cell contents were degassed with argon for 5 minutes during the first run and for 30 seconds between successive runnings. Voltammetric measurements were carried out after degassing with argon for 5 minutes. Voltammograms were then recorded by scanning the potential toward the positive direction on GCE (oxidation studies) and toward the negative direction on HMDE (reduction studies) versus the reference electrode.

A three-electrode combination system for bulk electrolysis (BE) was used. The system included a mercury pool (55.4 cm^2), a glassy sieve as working electrode, a coiled platinum wire as an auxiliary electrode [BAS MW-1033 (23 cm)], and Ag/AgCl as reference electrode (BAS MF-2052 RE-5B in 3.0 M KCl). In BE studies, 25 mL of 10 μM solutions were used for both electrodes.

2.4. Preparation of Cefnet tablets

Cefnet tablets were obtained from a local market in Amasya and were used as the dosage form obtained. Each tablet contains 600 mg CEF. Ten tablets were accurately weighed and crushed into a homogeneous fine powder in a mortar and mixed well. The average weight of one tablet was calculated. A powdered sample, equivalent to one tablet, was weighed and transferred into a calibrated flask containing approximately 100 mL of absolute ethanol. The contents of the flask content were then sonicated for 10 minutes. After standing at room temperature for approximately 30 minutes, the volume of this flask was increased to 250 mL by adding double-distilled water. Then, to prepare the final concentration, a required amount of sample from the clear supernatant liquor was withdrawn and quantitatively diluted with the supporting electrolyte solution. Quantitations in all proposed methods were performed by the calibration curve method from the related calibration equations.

2.5. Preparation of spiked human serum

Drug-free human serum samples were obtained from healthy volunteers and stored frozen until assay. After gently thawing the samples, 2.0 mL of an aliquot volume of serum sample was spiked with CEF in BR buffer to maintain 0.1 mM CEF concentration in serum, and acetonitrile was added to precipitate serum proteins. The mixture was then vortexed for 25 seconds

and centrifuged for 10 minutes at 5000g to eliminate serum protein residues. Approximately 2.0 mL mixture from the supernatant was taken and added into supporting electrolytes to attain a total volume of 10.0 mL. Sufficient volume (25, 50, 100, 200 μL, etc.) from this solution was taken and added to the voltammetric cell containing 10.0 mL of supporting electrolyte. Determination was performed as described in the "Preparation of Cefnet Tablets" section.

2.6. Computation

Theoretical calculations were performed to support the proposed mechanism for electrode processes. Such calculations were performed with the Gaussian 09 suite of programs [34]. Molecular geometry of CEF was fully optimized at the AM1 level. Frequency calculations were computed at the same level to verify that the optimized geometry is a real minimum on the potential energy surface without any imaginary frequency. Single-point energy calculation was performed using AM1-optimized geometry at the DFT/B3LYP level of theory, with the popular polarized basis set, 6-31+G (d), which adds d functions on heavy atoms.

3. Results and discussion

Electrochemical behavior, diffusion, and adsorption properties of CEF were studied at the HMDE on the reduction side and at the GCE on the oxidation side. In these studies, electrochemical methods such as cyclic voltammetry (CV), differential pulse voltammetry (DPV), square-wave voltammetry (SWV), and constant potential BE were used.

3.1. Electrochemical behavior of CEF on HMDE and GCE

In CV studies, on HMDE, two well-defined reduction peaks on negative scan at approximately −0.4 (PI) and −1.0 V (PII) in BR of pH 4.2 were observed (Fig. 2A), whereas a well-defined oxidation peak on the positive scan on GCE at approximately 0.9 V in BR of pH 5.0 was observed (Fig. 2B) Height of these peaks increased with increasing CEF concentration (Fig. 2C and D). Because no anodic peak on reverse scan on HMDE and no cathodic peak on reverse scan on GCE were observed, an irreversible nature for reduction on HMDE and oxidation on GCE could be suggested [27−33].
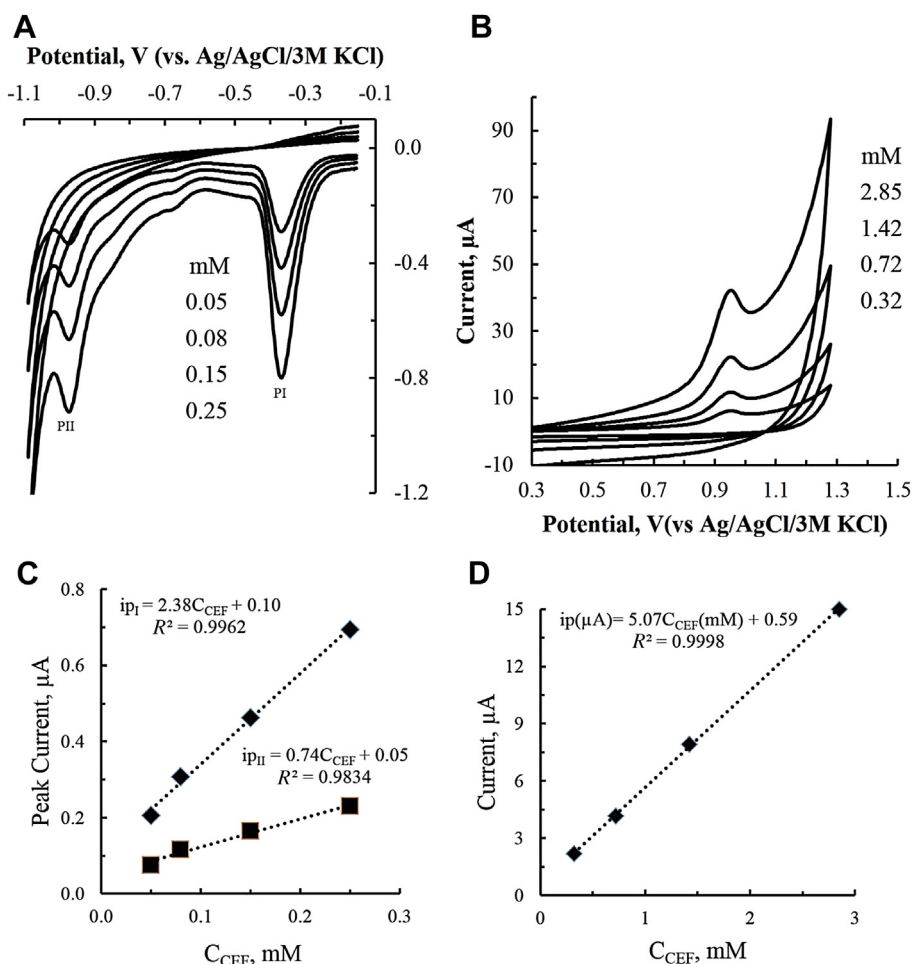
Fig. 2 − **Cyclic voltammograms of cefdinir (CEF) solutions at different concentrations on (A) hanging mercury drop electrode (HMDE) in Britton−Robinson (BR; pH 4.2) and (B) glassy carbon electrode (GCE) in BR (pH 5.0); scan rate = 0.100 V/s. (C and D) Dependency of peak current on CEF concentration for HMDE and GCE, respectively.**

The electrochemical behavior was studied in detail. As a first step, the effect of pH on peak potential and peak current was studied using SWV on HMDE and using CV on GCE between pH 2.0 and 12.0. As could be seen from Fig. 3A, reduction potentials of both peaks on HMDE shifted to more negative potentials with increasing pH between 2.0 and 7.5 (to avoid making the figure more confusing and complicated, only 3 of 6 square-wave voltammograms were given). This may be due to the initial protonation of a functional group followed by electron transfer. It is clear that the lower the pH (higher H_3O^+ concentration), the more easily the functional group can be protonated and the less potential is needed for reduction. Reduction peaks were not observed at pH values higher than 8.0 on HMDE. By contrast, potential of oxidation on GCE is pH independent between pH 2.0 and 5.0 and 8.0 and 12.0, and it was observed to shift to less potential values with increasing pH between 5.0 and 8.0 (Fig. 3B). This behavior may be explained as follows: The functional group that is going to be oxidized is fully protonated at lower pHs and is fully deprotonated at higher pHs, and as a result, peak potential is independent of pH. Change in potential with pH could be concluded as an evidence of protonation and shifting of peak potential to less positive potentials with increasing pH may be concluded as a deprotonation step before electron transfer.

Subsequently, the graph of pH versus E_p was constructed for both electrodes and the peak potential was found to change linearly with the pH obeying the equation for PI on HMDE: E_{pI} (V) $= -0.042$ pH $- 0.28$ ($R^2 = 0.9987$) and for PII on HMDE E_{pII} (V) $= -0.047$ pH $- 0.88$ ($R^2 = 0.9984$; Fig. 3C). Oxidation process has the following pH versus E_p behavior: E_p (V) $= -0.047$ pH $+ 1.28$ ($R^2 = 0.9998$; Fig. 3D) The *slope* of these graphs should be equal to $2.303RT\partial/nF$, where ∂ is the number of protons involved in the electrode reaction, n is the number of electrons transferred, and the rest are commonly known constants [33]. In this study, ∂/n values were calculated as 0.7, 0.8, and 0.8, for PI, PII on HMDE, and oxidation peak on GCE, respectively. These values represent the transfer of same number of electrons and protons in the reduction mechanisms on HMDE and oxidation on GCE. Peak current, peak shape, and symmetry were taken into account, and finally the optimal pH was selected as 4.2 for HMDE and 5.0 for GCE.

Afterward, the effect of scan rate on peak potential was investigated while CEF concentration was held constant at 0.1 mM for HMDE and 2.5 mM for GCE. It is clear from Fig. 4A and B that the potentials of both reduction processes on HMDE and potential of oxidation on GCE change with the scan rate. Changing of the potential with scan rate should be explained by quasireversible or irreversible mechanism [27−30]. As
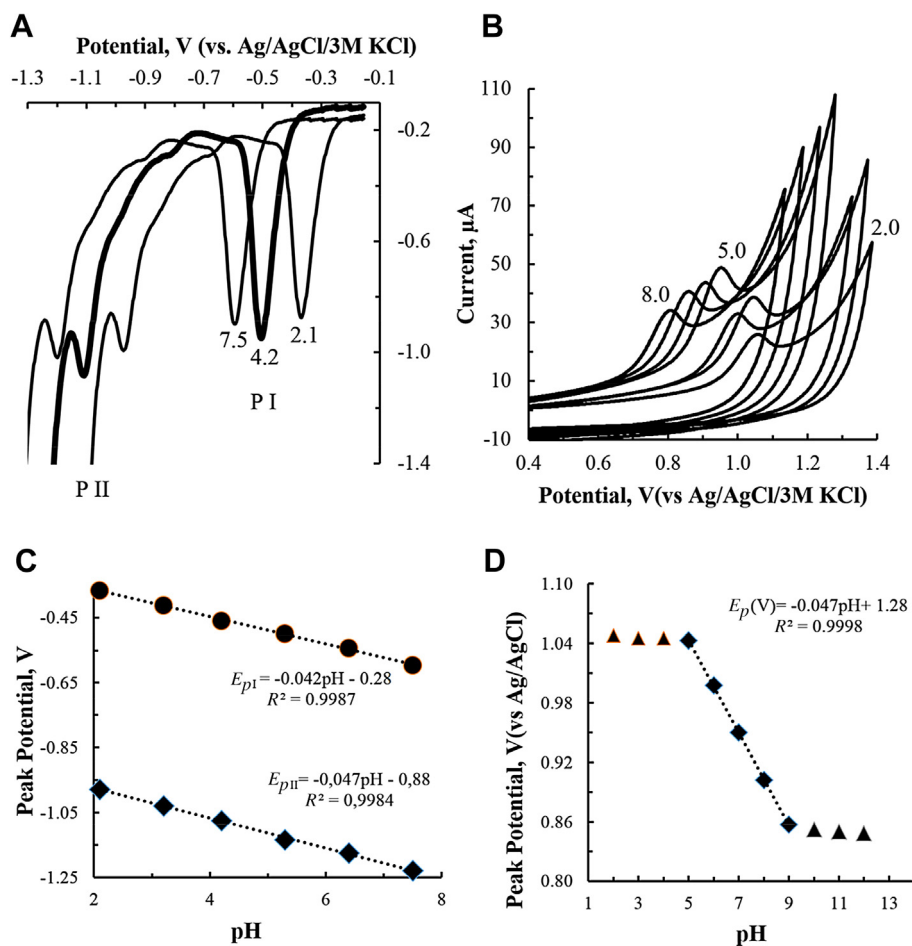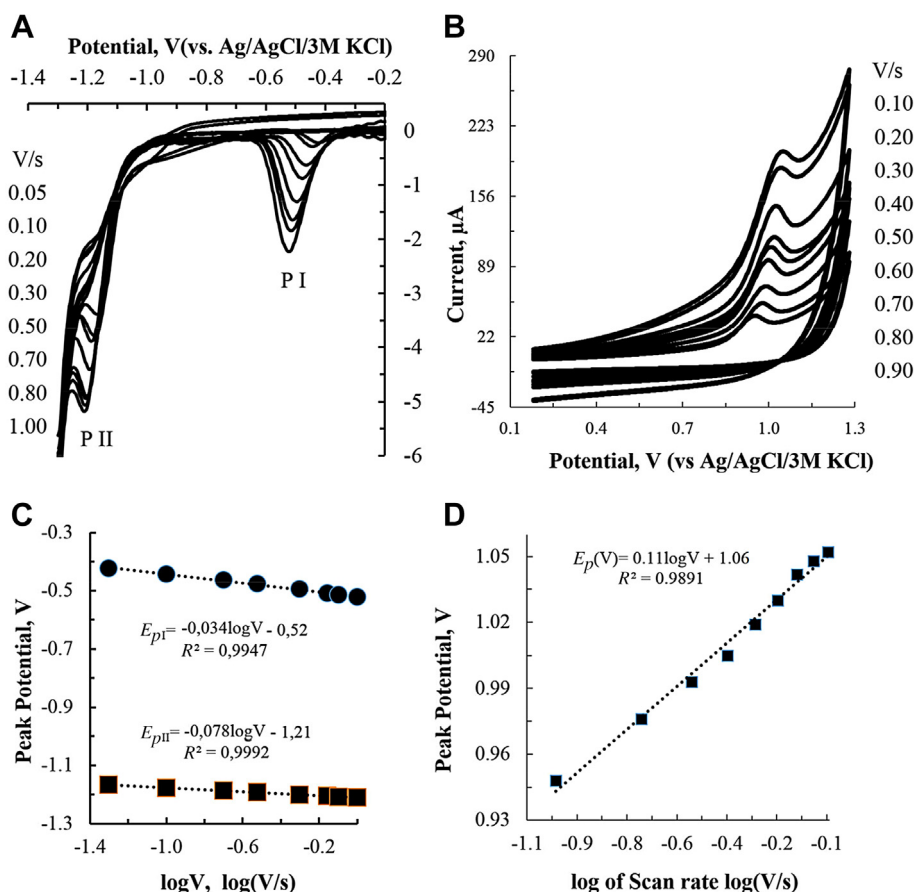

Fig. 3 − Effect of pH on peak current and peak potential on (A) hanging mercury drop electrode and (B) glassy carbon electrode. (C and D) Peak potential versus pH.

Fig. 4 — Influences of scan rate on peak current and peak potential on (A) hanging mercury drop electrode (HMDE), (B) glassy carbon electrode (GCE) in Britton—Robinson of optimum pHs for C_{CEF} of (A) 0.1mM and (B) 2.5mM. (C and D) Peak potential versus logarithm of scan rate for HMDE and GCE, respectively.

given in Fig. 4C and D, peak potential versus logarithm of scan rate was figured out, and the slope of these straight lines were used to calculate the value for α (charge transfer coefficient). Value for αn, where n is number of electrons, was calculated as 1.74 for PI, 0.76 for PII on HMDE, and 0.53 for GCE.

The effect of scan rate on peak current was also studied. Peak current of PI on HMDE changes linearly with increasing scan rate, whereas that of PII is not linear (Fig. 5A). The graph of peak current versus square root of scan rate was found to be linear for PII, whereas for PI, this relation was not linear (Fig. 5B). More importantly, slope of the plot of logarithm of peak current versus logarithm of scan rate was found to be 0.71 for PI and 0.24 for PII (Fig. 5C). As a result, reduction at PI should be a surface confined process and reduction at PII should be a diffusion controlled (electrode—solution interface) processes [27—33]. Parallel studies were performed for oxidation on GCE and it was found that peak current changes linearly with scan rate (Fig. 5D), logarithm of peak current changes with logarithm of scan rate by the slope value of 0.83 (Fig. 5E), and peak current has no linear dependency to square root of scan rate (Fig. 5F). This observation may be explained by the effect of adsorption on the oxidation mechanism.

BE studies at −0.8 and −1.5 V were carried out to find the number of electrons in the two reduction mechanisms on

HMDE and at 1.4 V for that of GCE. After BE, Faraday equations were used to calculate the number of electrons and it was found to be four for PI on HMDE, two for PII on HMDE, and one for oxidation peak on GCE.

3.2. Theoretical investigation

An electron flows from the metal electrode into the lowest unoccupied molecular orbital (LUMO) of the molecule as reduction takes place. When oxidation occurs, the electron from the highest occupied molecular orbital (HOMO) is involved. Consequently, the arrangement of these frontier molecular orbitals is important to determine the most relevant part/atoms of the molecule for redox reactions. It is therefore necessary to determine the HOMO—LUMO of the molecule to support the reduction and oxidation mechanism in a more accurate way. For this reason, to predict HOMO and LUMO, CEF geometry was optimized first, using semiempirical methods (AM1). These methods are fast but often fail to predict accurate energy values of compounds. Therefore, a more accurate basis set was found necessary to obtain energy values that match experimental accuracy. Accordingly, single-point energy calculation processes were performed at B3LYP/6-31+G (d). HOMO and LUMO together with their corresponding energies are depicted in Fig. 6.
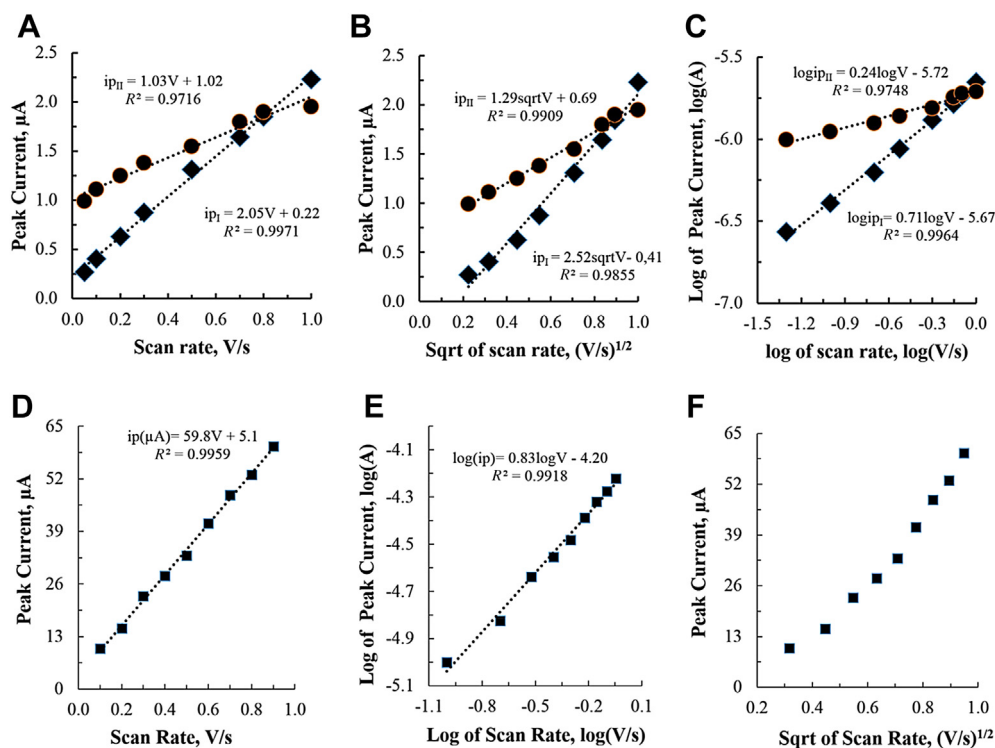
Fig. 5 – (A) i_p versus scan rate; (B) i_p versus square root of scan rate; (C) logarithm of peak current versus logarithm of scan rate for hanging mercury drop electrode; (D) i_p versus scan rate; (E) logarithm of peak current versus logarithm of scan rate; (F) i_p versus square root of scan rate for glassy carbon electrode.

According to Fig. 6, less tightly held electrons in the molecule (HOMO) lie mainly on the five-membered ring containing nitrogen and sulfur. Aminothiazolyl groups are known to be oxidized by one electron, which causes dimerization. The related mechanisms are postulated in the literature [33]. The reported oxidation mechanism is irreversible, which was initiated by removal of proton from the five-membered, S- and N-containing ring, followed by a transfer of electron, and finally dimerization. Therefore, the oxidation of CEF is also expected to proceed in the same way that agrees well with both theoretical and experimental findings. As a result, the mechanism figured out in Scheme 1A is proposed for oxidation reaction.

Because there are different functional groups on CEF that are available to be reduced, several reduction mechanisms may be proposed. First of all, according to experimental results, there is one reduction with $4e^-$ and $4H^+$ at the same potential and another one with $2e^-$ and $2H^+$ at higher potential than the first one, and both reductions are irreversible. The first possible reduction may be protonation of the carboxylic oxygen first, followed by electron transfer. This mechanism is also supported by computational study, which shows that the reduction centers are located around carbonyl oxygen groups. In this mechanism, before electron transfer, protonation of carbonyl oxygen takes place first, indicating that this is a classical acid-catalyzed reaction. The reduction of carbonyl group will be more favorable at low pHs and needs lower potential. Similarly, protonation step will be more difficult in higher pHs and higher potential will be needed as
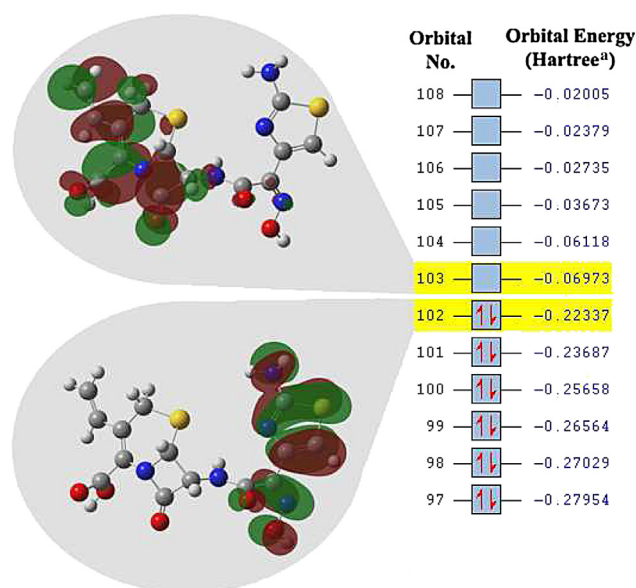
Fig. 6 – Frontier molecular orbitals mapped on optimized molecular structure of cefdinir, and their corresponding energies calculated at B3LYP/6-31+G (d)//AM1 and contribution of atoms to highest occupied molecular orbital and lowest unoccupied molecular orbital. *1 Hartree = 1 a.u. = 27.211 eV = 2626kj/mol.
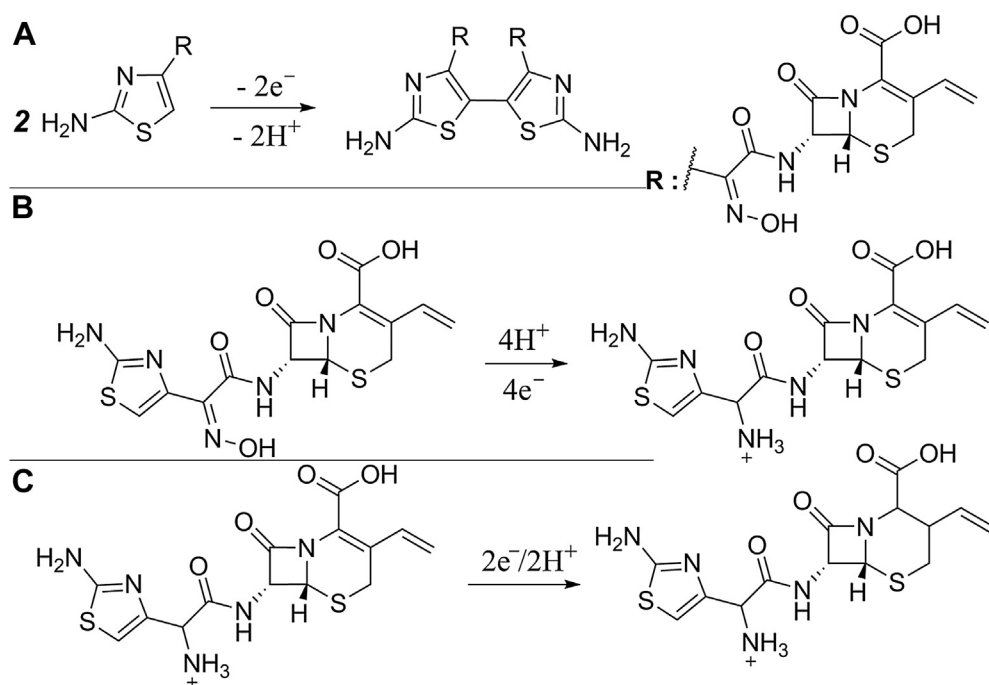
Scheme 1 – Proposed mechanisms for cefdinir: (A) oxidation on glassy carbon electrode; (B) reduction for PI on hanging mercury drop electrode (HMDE); (C) reduction for PII on HMDE.

investigated in pH studies, but again, reduction of carbonyl oxygen needs two electrons, which will not fit with the experimental findings of this study. Reduction of two similar oxygen groups may be the plausible one, but at this time reductions should take place at different potentials because they have completely different relative energies, and this investigation does not meet the study's expectation. To meet the experimental results, there should be four electrons and four protons. If the reduction of two same groups with different environments and different location and of course different relative energies is thought to be possible at the same potential, then it is plausible to propose that the reduction mechanism for PI involves the reduction of two carbonyl oxygen to corresponding alcohols. Otherwise, it is possible to reduce only one group with participation of four electrons and four protons for PI on HMDE and this mechanism is shown in Scheme 1B with the support of similar mechanisms in literature [18,19].

The reduction of unsaturated alkyne as proposed in the literature [18,19] may be the first possibility for PII. There is one more alternative to this mechanism that should not be disregarded: due to reduction of the unsaturated moiety of a six-membered ring, S and N atoms are located on the vicinity of the carboxylic group. High electronegativity of the N and S atoms and also the electron-withdrawing capability of the carboxylic group may activate the unsaturated moiety of the ring, and the mechanism presented in Scheme 1C may take place on PII.

Reduction and oxidation mechanisms were supported by the experimental studies about a similar molecule of the cephalosporin group. Even in this study, the electrochemistry of cefditoren pivoxil was investigated along similar lines. In this study, one reduction on HMDE with four electrons and four protons and one oxidation with one electron and one

proton were observed. According to these results, oxidation of CEF on GCE and its reduction on HMDE take place at PI have the similar mechanism with those for cefditoren pivoxil. Beside, its reduction on HMDE takes place at PII might be the reduction of functional group that is not present in the structure of cefditoren pivoxil.

3.3. Voltammetric determination of CEF

In an effort to develop a voltammetric method for the determination of CEF, quantitation of peak current resulting from the reduction on HMDE and oxidation on GCE was examined. Square-wave (SWV) and differential pulse (DPV) techniques were applied first without using stripping mode. In such studies, DPV was found to be more suitable and reproducible than SWV for both electrodes. Then, due to the adsorptive behavior of CEF, to find more sensitive methods, differential pulse cathodic adsorptive stripping voltammetry for HMDE and differential pulse anodic adsorptive stripping voltammetry for GCE were applied.

The nature of supporting electrolyte affects the peak response of the CEF. Thus, various electrolytes such as BR, phosphate, and acetate buffer solutions were examined to find the optimum conditions for quantification of CEF. BR gave the highest peak current and better peak shape than the other buffers. Therefore, BR was selected for further studies. The effect of pH was also investigated. Peak current, peak shape, and peak symmetry were taken into account and then optimal pH was selected as 4.2 and 5.0 for HMDE and GCE, respectively, as emphasized before.

For all techniques, variation of peak current and its shape with instrumental conditions such as scan increment (ΔE_i), pulse amplitude (ΔE_a), pulse width (ΔE_w), accumulation time
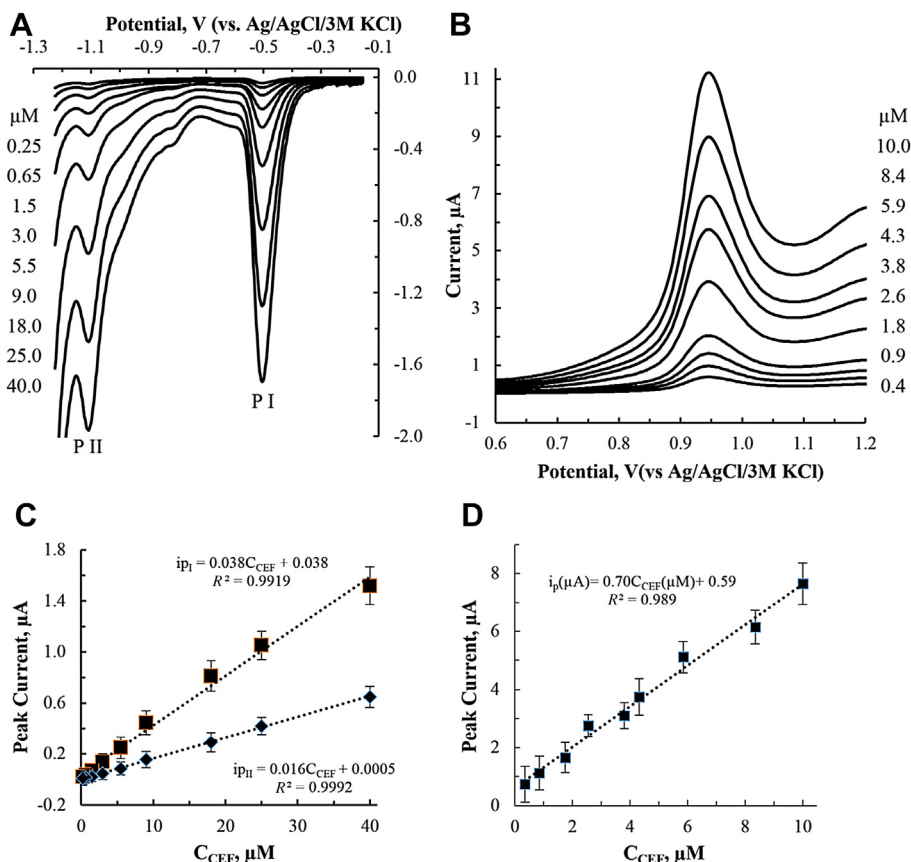
Fig. 7 – Calibration dependencies on (A) hanging mercury drop electrode (HMDE) and (B) glassy carbon electrode (GCE); calibration graphs for (C) HMDE and (D) GCE. CEF = cefdinir.

(t_{acc}), and accumulation potential (E_{acc}) were investigated using 1.5 μM CEF in BR at optimal experimental conditions. As a result, optimum instrumental parameters were found to be follows: $\Delta E_i = 3$ mV, $\Delta E_a = 65$ mV, $\Delta E_w = 0.01$ s; −0.15 V and 90 s were found as E_{acc} and t_{acc} for HMDE, respectively, and 0.60 V and 120 s for GCE.

Applying these optimized conditions, the applicability of the proposed voltammetric procedures for the determination of CEF was investigated. Peak currents were measured as a function of CEF concentration in quintuplicate under the optimized operational parameters and the average of these five serial measurements was used as a peak current. Calibration graphs for CEF were obtained to estimate the analytical characteristics of methods. Results are given in Fig. 7A for HMDE and Fig. 7B for GCE.

3.4. Validation of proposed methods and determination of CEF in tablets and human serum

The proposed voltammetric methods were validated by investigating the following parameters: linearity range, limits of detection (LOD) and limits of quantification (LOQ), accuracy, reproducibility, and repeatability according to the International Conference on Harmonisation guidelines [35].

Linearity was checked by preparing 15 standard solutions with different CEF concentrations for each electrode. Five

Table 1 – Regression data of the calibration curve.			
Regression parameter	HMDE PI	HMDE PII	GCE
Linearity range, μM	0.25–40.0	0.25–40.0	0.40–10.0
Slope of calibration curve, AL/mol	0.038	0.016	0.704
Intercept, nA	38.0	5.0	590
Standard deviation (SD) of regression, nA	51	6.7	270
SD of slope, AL/mol	0.001	0.0002	0.028
SD of intercept, nA	0.81	0.33	18
Limit of deduction, μM	0.063	0.061	0.079
Limit of quantification, μM	0.21	0.20	0.26
Determination coefficient, R^2	0.9919	0.9992	0.9890
Within-day repeatability of peak current[a], (% RSD)	7.65	8.25	10.25
Between-day repeatability of peak current[a], (% RSD)	9.12	10.52	13.58
Within-day repeatability of peak potential[a], (% RSD)	1.78	2.89	3.78
Between-day repeatability of peak potential[a], (% RSD)	2.98	4.68	5.12

GCE = glassy carbon electrode; HMDE = hanging mercury drop electrode; RSD = relative standard deviation.
[a] For five serial measurements.

Table 2 – Recovery of CEF from Cefnet tablets.

Electrode	Nominal value, mg	Values calculated, mg	Recovery[a], %	RSD[b], %
HMDE	600	542, 575, 592, 612, 645	98.9 ± 8.0	6.5
GCE	600	535, 585, 597, 625, 680	100.7 ± 11.1	8.8

CEF = cefdinir; GCE = glassy carbon electrode; HMDE = hanging mercury drop electrode.
[a] Value = average ± ts/$\sqrt{N}$ (N = 5 and at 95% confidence level).
[b] Relative standard deviation for five serial measurements.

serial measurements were taken for each concentration and subsequent to evaluation of the required statistical test (Q test), the average of measurements was used as a peak current of related concentration. The good linearity of the calibration graphs and the negligible scatter of the experimental points are clearly evident from the coefficient of determination (R^2; Fig. 7C and D).

The LOD and LOQ values of proposed methods were calculated using equations given in the literature [31–33], and the results are presented in Table 1. For the studies on HMDE, the method presents coefficient of determination (R^2) higher than 0.99 for both peaks. Repeatability and reproducibility of peak current and peak potential were found satisfactory in all methods. In case of GCE, the method presents R^2 higher than 0.98 but repeatability and reproducibility of peak current were slightly less satisfactory compared with HMDE. The proposed methods on both HMDE and GCE can be used for pharmaceutical preparations and biological fluids.

To evaluate the applicability of the proposed methods to pharmaceutical preparations and biological samples, CEF was determined in Cefnet tablets and spiked human serum samples. As shown in Table 2, the mean results of each application for both electrodes lie between 98.9% and 100.7 % (relative standard deviation < 10.0%) for tablet recovery. These results indicate the validity of proposed methods.

Recovery studies in spiked human serum samples were also performed. In these applications, voltammetric baseline for CEF-free serum samples in BR solution was taken and no voltammetric signal in the potential range of CEF was found. It was concluded that there is no interference effect of any potential species found in human serum. As could be seen in

Table 3, recovery values are approximately 98%. The differences between spiked and calculated concentrations are insignificant at the 95% confidence level.

4. Conclusion

Oxidation properties of CEF on GCE were characterized with the help of *ab initio* calculations for the first time and computational results were integrated to its reduction characteristics on HMDE. Redox properties and electrochemical parameters of drug molecules may be of crucial importance in understanding the mechanism of action against their target/related organs. The electrochemical reduction and oxidation of CEF on HMDE and GCE were proposed. Determination of drug molecules in pharmaceuticals and biological samples are also of great importance. In the present study, precise, accurate, rapid, and sensitive adsorptive stripping methods require neither sophisticated instrumentation nor tedious extraction processes have been proposed. Consequently, the proposed methods have the potential of a good analytical alternative for CEF determination in pharmaceutical formulations and human serum. In addition, they can be adopted for pharmacokinetic studies as well as for quality control laboratory studies.

Conflicts of interest

There is no conflict of interest regarding this paper.

Acknowledgments

Table 3 – Recovery of CEF from spiked human serum.

Electrode	Value spiked, μM	Value calculated, μM	Recovery[a], %	RSD[b], %
HMDE	0.52	0.46	98.6 ± 9.0	7.4
	1.15	1.10		
	2.0	2.13		
	3.0	3.15		
	6.65	6.49		
GCE	0.32	0.37	98.0 ± 14.9	12.2
	1.25	1.10		
	3.0	2.63		
	5.0	5.23		
	8.5	8.0		

CEF = cefdinir; GCE = glassy carbon electrode.
[a] Value = average ± ts/$\sqrt{N}$ (N = 5 and at 95% confidence level).
[b] Relative standard deviation for five serial measurements.

REFERENCES

[1] Inamoto Y, Chiba T, Kamimura T, et al. FK-482, a new orally active cephalosporin. Synthesis and biological properties. J Antibiot (Tokyo) 1988;41:828–30.

[2] Mine Y, Kamimura T, Watanabe Y, et al. *In vitro* antibacterial activity of FK482, a new orally active cephalosporin. J Antibiot (Tokyo) 1988;41:1873–87.

[3] Jin H-E, Kim I-B, Kim C-K, et al. Determination of CEF levels in rat plasma and urine by high-performance liquid chromatography-tandem mass spectrometry: application to pharmacokinetics after oral and intravenous administration of cefdinir. Biomed Chromatogr 2013;27:1423—30.

[4] Li J, Li W, Chen Z, et al. Development and validation of a rapid HPLC method for the determination of cefdinir in beagle dog plasma integrated with an automatic on-line solid-phase extraction following protein precipitation in the 96-well plate format. J Chromatogr B Analyt Technol Biomed Life Sci 2012;895:83—8.

[5] Okamoto Y, Itoh K, Namiki Y, et al. Method development for the determination of cefdinir and its related substances by high-performance liquid chromatography. J Pharm Biomed Anal 1996;14:739—48.

[6] Hashem H, Gouda AA, Hassan W. Development and validation of a rapid stability indicating chromatographic determination of cefdinir in bulk powder and dosage form using monolithic stationary phase. J Liq Chromatogr Relat Technol 2012;35:1638—48.

[7] Hamrapurkar P, Patil P, Phale M, et al. A developed and validated stability-indicating reverse-phase high performance liquid chromatographic method for determination of cefdinir in the presence of its degradation products as per International Conference on Harmonization guidelines. Pharm Methods 2011;2:15—20.

[8] Khan A, Iqbal Z, Khan MI, et al. Simultaneous determination of cefdinir and cefixime in human plasma by RP-HPLC/UV detection method: method development, optimization, validation, and its application to a pharmacokinetic study. J Chromatogr B Analyt Technol Biomed Life Sci 2011;879:2423—9.

[9] Sanli N, Sanli S, Sizir U, et al. Determination of pK$_a$ values of cefdinir and cefixime by LC and spectrophotometric methods and their analysis in pharmaceutical dosage forms. Chromatographia 2011;73:1171—6.

[10] Wu CS, Zhang JL, Qiao YL, et al. Simultaneous determination of 14 beta-lactam antibiotics in cosmetic products by liquid chromatography tandem mass spectrometry method. Chin Chem Lett 2011;22:334—7.

[11] Chen ZJ, Zhang J, Yu JC, et al. Selective method for the determination of cefdinir in human plasma using liquid chromatography electrospray ionization tandem mass spectrometry. J Chromatogr B Analyt Technol Biomed Life Sci 2006;834:163—9.

[12] Mehta TN, Subbaiah G, Pundarikakshudu K. Determination of cefdinir by a stability-indicating liquid chromatographic method. J AOAC Int 2005;88:1661—5.

[13] Hadad GM, Emara S, Mahmoud WMM. Optimization and validation of an LC method for the determination of cefdinir in dosage form and human urine. Chromatographia 2009;70:1593—8.

[14] Bano S, Mohd A, Khan AAP, et al. Resonance Rayleigh scattering spectra, nonlinear scattering spectra of selected cephalosporins-Cd(II) chelate with titan yellow and their analytical applications. J Dispers Sci Technol 2011;32:1023—31.

[15] Gouda AA, Hassem H, Hassan W. Spectophotometric methods for determination of cefdinir in pharmaceutical formulations via derivatization with 1,2-naphthoquinone-4-sulfonate and 4-chloro-7-nitrobenzo-2-oxa-1, 3-diazole. Drug Test Anal 2012;4:991—1000.

[16] Singh BK, Parwate DV, Srivastava S, et al. Selective and non-extractive spectrophotometric determination of cefdinir in formulations based on donor-acceptor complex formation. Quim Nova 2010;33:1471—5.

[17] Dong SY, Yu ZQ, Han XF, et al. Voltammetric behavior of degradation product and determination of cefdinir. Chem Res Chin U 2009;25:807—11.

[18] Jain R, Dwivedi A, Mishra R. Voltammetric behavior of cefdinir in solubilized system. J Colloid Interface Sci 2008;318:296—301.

[19] Jain R, Radhapyari K, Jadon N. Electrochemical evaluation and determination of cefdinir in dosage form and biological fluid at mercury electrode. J Electrochem Soc 2007;154:F199—204.

[20] Neves MMPS, Nouws HPA, Delerue-Matos C. Carbon surfaces for the oxidative quantification of pravastatin: glassy-carbon vs. screen-printed carbon electrodes. J Food Drug Anal 2010;18:353—7.

[21] Lencastre RP, Matos CD, Garrido J, et al. Voltammetric quantification of fluoxetine: application to quality control and quality assurance processes. J Food Drug Anal 2006;14:242—6.

[22] Pamuk D, Taşdemir IH, Ece A, et al. Redox pathways of Aliskiren based on experimental and computational approach and its voltammetric determination. J Brazil Chem Soc 2013;24:1276—86.

[23] Zorluoğlu SL, Taşdemir IH, Ece A, et al. A cooperative computational and experimental investigation on electrochemical behavior of metoprolol and its voltammetric determination. Can J Chem 2013;91:951—9.

[24] Solangi AR, Khuhawar MY, Bhanger MI. Adsorptive stripping voltammetric determination of fluoroquinolones in pharmaceuticals. J Food Drug Anal 2005;13:201—4.

[25] Chang ML, Chang CM. Simultaneous voltammetric determination of ascorbic acid and its derivatives in cosmetics using epoxy-carbon composite electrodes. J Food Drug Anal 2005;13:205—11.

[26] Wang J. Analytical electrochemistry. 2nd ed. New York: Wiley-VCH; 2000.

[27] Brett CMA, Brett AMO. Electrochemistry, principles, methods and applications. 3rd ed. Oxford, UK: Oxford University Press; 1996.

[28] Bard AJ, Faulkner LR. Electrochemical methods, fundamentals and applications. 2nd ed. Hoboken, NJ: John Wiley & Sons Inc.; 2001.

[29] Bond AM. Broadening electrochemical horizons. Oxford, UK: Oxford University Press; 2002.

[30] Duran M, Durmuş Z, Taşdemir IH, et al. Voltammetric stripping methods for direct determination of disopyramide. Curr Pharm Anal 2012;8:28—36.

[31] Erdoğan DA, Taşdemir IH, Erk N, et al. Electrochemical behavior of moclobemide at mercury and glassy carbon electrodes and voltammetric methods for its determination. Collect Czech Chem Commun 2011;76:423—42.

[32] Taşdemir IH, Ece A, Kılıç E. Experimental and theoretical study on the electrochemical behavior of zofenopril and its voltammetric determination. Curr Pharm Anal 2012;8:339—48.

[33] Frisch MJ, Trucks GW, Schlegel HB, et al. Gaussian 09, Revision C.01. Wallingford, CT: Gaussian, Inc.; 2009.

[34] Jouikov V, Simonet J. Electrochemical reactions of sulfur organic compounds. In: Bard AJ, Stratmann M, Scholz F, et al., editors. Encyclopedia of electrochemistry, Vol. 8. Weinheim, Germany: Wiley-VCH Verlag GmbH & Co.; 2007. pp. 235—71.

[35] International Conference on Harmonisation of Technical Requirements for Registration of Pharmaceuticals for Human Use. Topic Q2(R1): validation of analytical procedures: text and methodology; 2005 [last accessed 16.07.2013] to location http://www.ich.org/fileadmin/Public_Web_Site/ICH_Products/Guidelines/Quality/Q2_R1/Step4/Q2_R1__Guideline.pdf.